Resonance-enhanced x-ray multiple ionization of a polyatomic molecule

X. Li,[1,2,*] A. Rudenko,[1,†] T. Mazza,[3] A. Rörig,[3] N. Anders,[4] Th. M. Baumann,[3] S. Eckart,[4] B. Erk,[5] A. De Fanis,[3] K. Fehre,[4] R. Dörner,[4] L. Foucar,[6] S. Grundmann,[4] P. Grychtol,[3] A. Hartung,[4] M. Hofmann,[4] M. Ilchen,[3,7] Ch. Janke,[4] G. Kastirke,[4] M. Kircher,[4] K. Kubicek,[3,8] M. Kunitski,[4] S. Meister,[9] N. Melzer,[4] J. Montano,[3] V. Music,[3,7] G. Nalin,[4] Y. Ovcharenko,[3] Ch. Passow,[5] A. Pier,[4] N. Rennhack,[3] J. Rist,[4] D. E. Rivas,[3] I. Schlichting,[6] L. Ph. H. Schmidt,[4] Ph. Schmidt,[3,7] M. S. Schöffler,[4] J. Siebert,[4] N. Strenger,[4] D. Trabert,[4] F. Trinter,[4,5,10] I. Vela-Perez,[4] R. Wagner,[3] P. Walter,[2] M. Weller,[4] P. Ziolkowski,[3] A. Czasch,[4] M. Meyer,[3] T. Jahnke,[3] D. Rolles,[1] and R. Boll[3,‡]

[1] *J.R. Macdonald Laboratory, Department of Physics, Kansas State University, Manhattan, Kansas 66506, USA*
[2] *Linac Coherent Light Source, SLAC National Accelerator Laboratory, Menlo Park, California 94025, USA*
[3] *European XFEL, Holzkoppel 4, 22869 Schenefeld, Germany*
[4] *Institut für Kernphysik, Goethe-Universität, Max-von-Laue-Strasse 1, 60438 Frankfurt am Main, Germany*
[5] *Deutsches Elektronen-Synchrotron (DESY), Notkestrasse 85, 22607 Hamburg, Germany*
[6] *Max-Planck-Institut für medizinische Forschung, 69120 Heidelberg, Germany*
[7] *Institut für Physik und CINSaT, Universität Kassel, Heinrich-Plett-Strasse 40, 34132 Kassel, Germany*
[8] *The Hamburg Centre for Ultrafast Imaging, 22761 Hamburg, Germany*
[9] *Max-Planck-Institute for Nuclear Physics, 69117 Heidelberg, Germany*
[10] *Molecular Physics, Fritz-Haber-Institut der Max-Planck-Gesellschaft, Faradayweg 4-6, 14195 Berlin, Germany*

(Received 5 February 2022; revised 9 March 2022; accepted 15 April 2022; published 2 May 2022)

Extremely high charge states of atoms and molecules can be created when they are irradiated by intense x-ray pulses. At certain x-ray photon energies, electron ejection from atoms can be drastically enhanced by transient resonances created during the sequential ionization process. Here we report on the observation of such resonance effects in a molecule, CH_3I, and show the photon-energy-dependent shift of resonance-induced structures in ion charge state distributions. By comparing the ion charge state distribution of CH_3I with that from ionization of atomic xenon, molecule-specific features are observed, which can be attributed to ultrafast intramolecular charge rearrangement. In addition, we experimentally demonstrate that the charge-rearrangement-enhanced x-ray ionization of molecules, previously found with hard x rays, also plays a role in the soft x-ray regime.

DOI: 10.1103/PhysRevA.105.053102

I. INTRODUCTION

Tightly focused femtosecond pulses generated by an x-ray free-electron laser (XFEL), with the intensity typically on the order of 10^{18} W/cm^2 or beyond, can eject multiple electrons from atoms and molecules. In the parameter range explored so far, such interaction is typically dominated by sequential multiphoton absorption and subsequent relaxation processes like Auger-Meitner decay [1–3]. Assuming sufficiently high photon flux, the highest ion charge state created is usually the last ionic charge state that can be reached before its ionization potential rises above the photon energy. However, if inner-shell electrons can be resonantly excited to high-lying orbitals, even higher charge states can be reached via subsequent autoionization of multiply excited states or by the absorption of an additional x-ray photon [4–7]. The production of such charge states can be complemented by ionization of intermediate excited states populated by electron-correlation effects [8,9].

In molecules, x-ray ionization is often strongly localized at the atomic sites with the largest photoabsorption cross sections. It is typically accompanied by subsequent charge redistribution and molecular fragmentation [10–15].

Understanding the atomic and molecular responses to intense x-ray pulses is of fundamental importance for XFEL-based applications. For example, the strong ionization by XFEL pulses is the source of sample damage [16,17] in coherent imaging experiments, which ultimately affects the resolution and interpretation of diffraction patterns.

Resonant excitation with intense x-ray pulses has been a topic of continuing research interest, largely because it can bring about a rich spectrum of intriguing physical phenomena including the Auger-Meitner process modified by Rabi cycling [18,19], ultraefficient ionization of high-Z atoms [4,5,7], creation of double-core-hole states [20], and resonance-enhanced multiphoton ionization in the x-ray regime [21]. In addition, it is the first step in novel XFEL-based techniques such as stimulated x-ray Raman scattering [22–24] and atomic inner-shell x-ray lasers [25]. In extended systems such as nanoclusters, transient resonances have been identified as one of the key factors for optimizing the imaging performance in x-ray diffraction experiments [26].

*xiangli@slac.stanford.edu
†rudenko@phys.ksu.edu
‡rebecca.boll@xfel.eu

Here we report the observation of resonance-enhanced x-ray multiple ionization of a molecule—iodomethane (CH_3I). Resonant excitation enables the creation of extremely high charge states which are otherwise not reachable. A shift of the resonance structure in the charge state distribution (CSD) is observed when changing the photon energy. These findings are supported by orbital energy-level calculations with the Hartree-Fock method [27,28]. By comparing the CSDs of iodine from ionization of CH_3I with the corresponding ones from ionization of its atomic counterpart xenon, features specific to the molecular case are observed, which can be explained by ultrafast charge rearrangement. In addition, charge-rearrangement-enhanced x-ray ionization of molecules (CREXIM), which can facilitate the creation of much higher total molecular charge states than expected from the independent-atom model, was discovered previously with hard x rays [14] and theoretically predicted with soft x rays [29]. Our experimental data confirms that CREXIM is also important in the soft x-ray regime.

II. EXPERIMENT

The experiment was carried out at the Small Quantum Systems (SQS) instrument at the European X-ray Free-Electron Laser facility [30]. X-ray pulses with a nominal duration of 25 fs were focused to a $\sim$1.5 μm spot size at the center of a COLTRIMS (Cold Target Recoil Ion Momentum Spectroscopy) reaction microscope [31–37], where they interacted with CH_3I molecules delivered by a supersonic gas jet assembly. A 30-μm-diameter nozzle is followed by three skimmers and an adjustable collimator; the distance from the nozzle to the interaction region is $\sim$54 cm. The chamber pressure was 1×10^{-10} mbar. The European XFEL, operated at a base repetition rate of 10 Hz, provided bursts of electron pulses at 1.1 MHz, out of which we used every sixth pulse to generate x-ray pulses for our experiment, that is, the photon pulses had a spacing of 5.5 μs, limited by the flight times of the heaviest ionic fragments. Thus the effective repetition rate of the experiment was 700 Hz. The ion fragments from the interaction were then guided by the spectrometer field to a time- and position-sensitive 120-mm-diameter detector with hexagonal delay-line readout [38], which allows reconstruction of the momentum vectors of the coincident ions. The experiment was repeated at three different photon energies, 2 keV, 1.5 keV, and 1.2 keV, with corresponding pulse energies of 1 mJ, 1.6 mJ, and 2.4 mJ at the interaction region. Data from the ionization of xenon under identical conditions were recorded as a reference for the molecular data. Xenon was chosen because it has a similar electronic structure and hence similar resonant enhancement as atomic iodine. For all three photon energies, x-ray ionization of CH_3I molecules is mostly localized at the iodine site, which has a photoabsorption cross section at least 50 times larger than that of the methyl group.

III. RESULTS AND DISCUSSION

Figure 1(a) shows the CSDs of iodine and carbon ions detected in coincidence from the x-ray ionization of CH_3I molecules at the three different photon energies. At all three photon energies, higher carbon ion charge states are more likely to be detected in coincidence with higher iodine ion

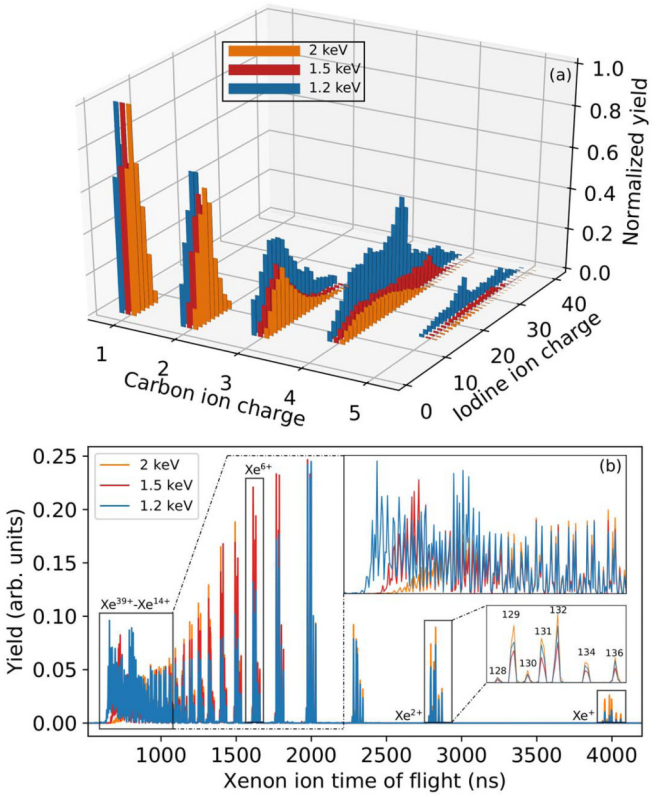

FIG. 1. (a) Charge state distributions of [I^{m+}, C^{n+}] ion pairs produced by ionization of CH_3I molecules with x rays at 2 keV, 1.5 keV, and 1.2 keV. The normalization is performed by scaling the maximum yield value of the charge state distribution to one. (b) Time-of-flight spectra of xenon ions produced by ionization of xenon atoms with x rays under the same conditions as in the molecular case. The inset at the top right magnifies the region of high charge states above Xe^{14+}. The seven Xe^{2+} peaks and their associated isotope masses (in amu) are shown by the inset at the bottom right. Also labeled are Xe^{+} and Xe^{6+} peaks.

charge states. This correlation is caused by the methyl group being in close vicinity of iodine while the latter is charged up by the ultrashort x-ray pulse, which allows efficient charge redistribution from iodine to the methyl group [10,11]. More charge transfer, which corresponds to higher carbon ion charge states, can occur with higher iodine ion charge states as predicted by the classical over-the-barrier model [39,40]. An increased yield of high charge states for lower photon energy is observed in Fig. 1. This is mainly caused by the larger pulse energies (hence higher fluences) that were delivered by the accelerator at smaller photon energies, which together with the larger absorption cross sections increase the photoaborption probability for each of the sequential ionization steps. It makes a comparison gated on the same pulse energy window infeasible. The influence of the pulse-energy and photon-energy changes on CREXIM and resonance-enhanced ionization, which can also contribute to the yield difference across the three different photon energies, will be discussed further below. Xenon ion time-of-flight spectra recorded under identical conditions are plotted in Fig. 1(b), with the region of high charge states from Xe^{14+} to Xe^{39+} enlarged in the inset

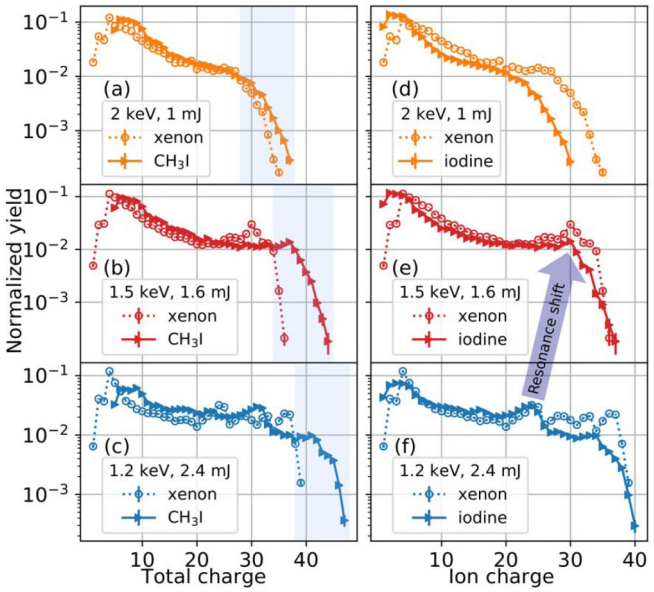

FIG. 2. Ion CSDs from x-ray ionization of xenon atoms and CH_3I molecules. The distributions are normalized to an integral of 1. Panels (a)–(c) show the total molecular CSDs of CH_3I in comparison with xenon. The light-blue shaded regions indicate the range of molecular charge states most affected by the CREXIM effect. The total molecular charge is obtained by summing up the carbon and iodine charges measured in coincidence as shown in Fig. 1(a) and adding the average hydrogen charge. Panels (d)–(f) show the CSDs of iodine from CH_3I in comparison with the same xenon data. The purple arrow indicates the shift of resonant enhancement as the photon energy changes from 1.2 keV to 1.5 keV

at the top right. Each of the charge state peaks consists of seven detectable xenon isotopes of masses (in amu): 128, 129, 130, 131, 132, 134, and 136 (see inset at the bottom right). At high charge states, the flight times of different isotopes of neighboring charge states start to overlap. A deconvolution based on the isotopic abundance is applied to these time-of-flight spectra in order to obtain the xenon CSDs shown in Fig. 2. In order to eliminate the effect of pulse energy fluctuations across the experimental runs and for a fair comparison between the molecular and atomic cases, all data are filtered on specific pulse energy windows and weighted according to the pulse energy distributions with a procedure previously discussed in the Supplemental Material of Ref. [15].

The CSDs for xenon and CH_3I are plotted in Fig. 2. The left column shows the comparison between the CSDs of the total molecular charge of CH_3I with those of xenon. The total molecular charge is obtained by summing up the carbon and iodine charges measured in coincidence as shown in Fig. 1(a) and adding the average hydrogen charge. For iodine charge states above 5+, we find by momentum conservation that all three hydrogens are always charged. For lower charge states, the average hydrogen charge increases from ∼2 to 3 [see Fig. 1(b) of Ref. [36]]. For all three photon energies, the total molecular CSD extends to higher charge states than that of xenon, and the yield of the highest charge states (light-blue shaded regions in Fig. 2) is enhanced in the molecular case relative to the atomic CSDs. Previous studies with lower x-ray intensities [10–13] have shown that the total molecular CSDs are very similar to the ones measured for their atomic counterpart, but with more intense hard x rays [14]; much higher total molecular charge states can be created because of charge-rearrangement-enhanced ionization. Our present observation with larger intensities than those in Refs. [10–13] confirms that CREXIM can be as important in the soft x-ray regime, and can increase the highest total charge state of a molecule in comparison to the atomic case. In the current work, this enhancement is larger at lower photon energy, with the charge difference between the highest charge states of CH_3I and xenon increasing from ∼2 at 2 keV to ∼7 at 1.2 keV. This is likely due to increased pulse energy from 1 mJ to 1.6 and 2.4 mJ (corresponding to a fluence increase from 1.8×10^{12} photons/μm^2 to 3.8 and 7.1×10^{12} photons/μm^2), and the increased photoabsorption cross section at lower photon energy, which can increase the ionization enhancement due to CREXIM, as was previously predicted for 8.3 keV x rays [14]. Although ionization is enhanced in the molecular case at all three photon energies, some of the charges created by the enhanced ionization of iodine are transferred to the methyl group, which results in a lower yield of high charge states in iodine than in xenon when the CREXIM enhancement is weaker, as shown in Fig. 2(d) for the 2 keV data.

When comparing the total molecular CSDs (left column of Fig. 2) and the iodine ion CSDs (right column of Fig. 2) with the xenon distributions, it is noticeable that the xenon CSD resembles the total molecular CSD at 2 keV [Fig. 2(a)], but is more similar to the iodine ion CSDs at 1.5 and 1.2 keV [Fig. 2(e) and Fig. 2(f)]. This can be attributed to the fact that charge-rearrangement-enhanced ionization has a larger effect in the 1.5 and 1.2 keV data than that of 2 keV, because of the larger photoabsorption cross section and higher pulse energies being used in the former cases. In the following, we first discuss some common features observed for both xenon and CH_3I in Figs. 2(a), 2(e) and 2(f), before identifying specific molecular effects in the charge state distributions at 1.2 and 1.5 keV. At 1.2 keV, the photons mainly interact with the M-shell (principal quantum number $n = 3$) electrons. The resonance-enhanced ionization is illustrated in Fig. 3 based on the calculated energy levels of iodine ions at different charge states. When iodine is ionized to I^{8+}, I^{14+}, and I^{21+}, the ionization thresholds of $3s$, $3p$, and $3d$ electrons surpass the photon energy. Starting from these charge states, the electrons occupying the orbitals with $n = 3$ can be resonantly excited to densely packed Rydberg states shown in light sky blue and high-lying unoccupied orbitals with principal quantum numbers $n = 5$, 6, and 7. These resonantly excited electrons can initiate Auger-Meitner processes, ejecting more electrons out of the molecule. In addition, the electrons deexcited to the N ($n = 4$) shell can be further ejected by direct photoionization. The resonant-excitation region ends at about I^{39+}, above which the $3p$ electrons cannot be energetically photoexcited to the $4s$ orbital, which is consistent with the extremely low yield of the highest charge state I^{40+} in Fig. 2(f). Note that when the $3d$ to $4f$ transition becomes energetically possible at I^{37+}, no $3d$ electrons are left in the ground-state configuration as indicated by the open dots in Fig. 3. Only excited-state configurations with electrons in the $3d$ orbital or decay processes filling electrons into the $3d$ holes can make transitions from

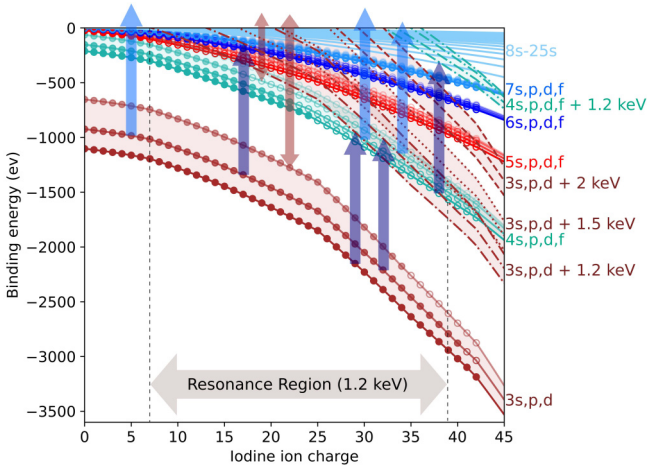

FIG. 3. Iodine ion binding energy at different charge states and illustration of the resonance-enhanced ionization for x rays at 1.2 keV. The binding energy values are calculated by the Hartree-Fock method including relativistic corrections with Cowan's atomic code [27,28]. The light blue arrows represent photoionization, the dark blue arrows represent resonant excitation, and the brown double arrows represent the Auger-Meitner process. The closed dots indicate electrons and open dots indicate electron holes in the ionic ground state at a given charge state. The energy levels for the $n = 3$ orbitals shifted by 1.2 keV, 1.5 keV, and 2 keV are shown by the dot-dashed, dotted, and dashed lines in dark red. The energy levels for the $n = 4$ orbitals shifted by 1.2 keV are shown by the dot-dashed lines in cyan.

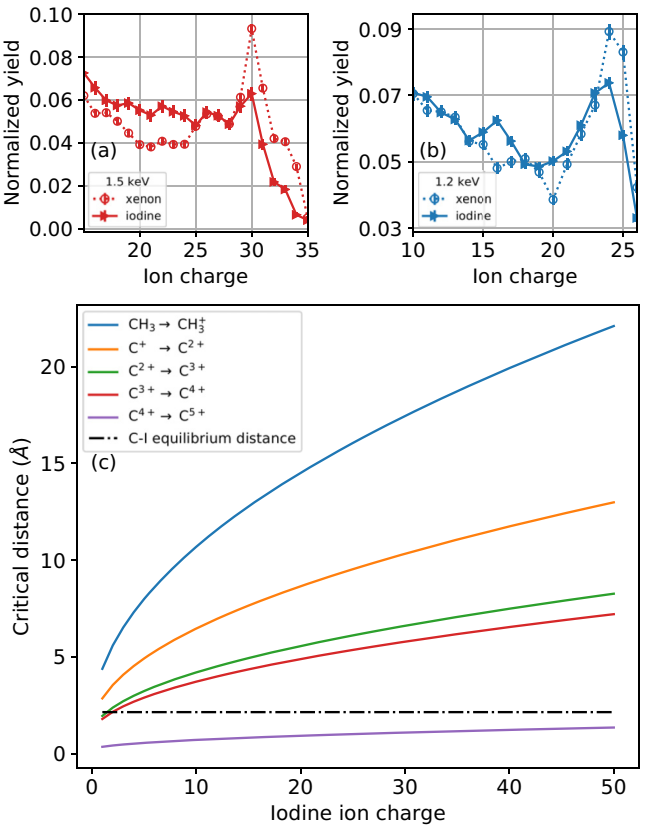

FIG. 4. (a) Ion CSDs near the resonant-enhancement regions for (a) 1.5 keV and (b) 1.2 keV. The CSDs are normalized such that the area under the curve is equal to 1. (c) Calculated critical distances for charge transfer from the iodine site to the methyl group or carbon ions. The C-I equilibrium bond length of 2.14 Å [41] is indicated as a dot-dashed black line.

$3d$ to $4f$ or $4p$ orbitals possible for these charge states above 37+. The dependence of the M-shell ($n = 3$) electron energy level on the charge state is also reflected in the structures of xenon and iodine CSDs. For example, the yield decreases at around I^{25+} because, at I^{24+}, $3p$ electrons cannot be excited to the $5d$ orbital anymore and, at I^{26+}, they cannot be excited to the $5s$ orbital.

At 1.5 keV, the resonant enhancement can be explained similarly as for 1.2 keV, except that the degree of enhancement at different charge states changes because the photon energy is changed. While the charge state region maximally enhanced by resonant excitations is at ∼23+ for 1.2 keV x rays, it is shifted to ∼30+ for 1.5 keV as illustrated by the light purple arrow in Fig. 2. In addition, the resonant excitation from $n = 3$ to $n = 4$, which is possible at 1.2 keV, does not contribute at 1.5 keV, because such excitation only becomes possible at very high charge states (I^{41+}), which cannot be reached under the fluence conditions of this experiment. With previous ejections, the highest charge state reachable is I^{37+} at which the resonant excitation from $3d$ to $5p$ is not possible anymore. I^{37+} matches well with the measured highest charge states as shown in Fig. 2(e). According to the energy levels in Fig. 3, direct ionization of the M-shell electrons by 2 keV x rays closes at I^{32+}. Electron ejections induced by resonant excitation extend the highest charge state to 37+ as shown in Fig. 2(a), at which the excitation from $3p$ to $6s$ orbitals is closed.

Despite the general resemblance between iodine ion CSDs and those of xenon in Figs. 2(e) and 2(f), molecule-specific features can be discerned at some particular charge states, which are highlighted in Figs. 4(a) and 4(b). At 1.5 keV, the major enhancement region for both iodine and xenon CSDs is around I^{30+} as shown in Fig. 4(a). About six charge states lower, i.e., starting from I^{24+}, a new, albeit weak, enhancement region specific to the iodine ion CSD appears. A similar observation can be made at 1.2 keV in Fig. 4(b), where the major enhancement region for both the atomic and molecular cases is around I^{24+}. About seven charge states lower, i.e., starting from I^{17+}, a new small peak appears for the iodine CSD, but not for xenon. These molecule-specific enhancement regions can be attributed to ultrafast charge rearrangement during the x-ray ionization of molecules. Based on the classical "over-the-barrier" charge-transfer model [39,40], the critical C-I distances beyond which charge transfer is forbidden are displayed together with the C-I equilibrium bond length of 2.14 Å [41] in Fig. 4(c). For electron transfer from CH_3, C^+, C^{2+}, and C^{3+} to iodine ions (with charge states above 1+), the critical distances are larger than the C-I equilibrium bond length, indicating that charge transfer is possible. However, electron transfer from C^{4+} is classically forbidden for all iodine charge states, as the critical distances are smaller than the C-I equilibrium bond length. Since electron transfer is the major pathway for carbon to acquire charges, the calculation is consistent with the very low yield of C^{5+} in Fig. 1(a), which we attribute to direct photoionization of C^{4+}. Therefore, the total number of

electrons transferable from the methyl group to iodine is seven, consisting of four electrons of carbon and three electrons from the three hydrogens. If iodine is not in the molecular environment, there would only be one resonant-enhancement region at around I^{30+} and I^{24+} for 1.5 keV and 1.2 keV, respectively. But when iodine is in the CH_3I molecular environment, it can receive seven or less electrons from the methyl group, which results in the development of molecule-specific enhancement regions located at about seven charge states lower than the major enhancement peaks present in both the atomic and molecular CSDs. We propose that the coexistence of both enhancement regions at the low (molecule-specific) and high (present in both atomic and molecular cases) charge states in the iodine CSD is caused by the variable timing of the charge rearrangement process relative to the XFEL pulse. If the charge redistribution occurs early, the reduced iodine ion charge states can be increased by the continued ionization of the XFEL pulse, with some of the final charge states ending up in the higher enhancement region. On the other hand, if the charge redistribution occurs late, the XFEL pulse has no time left to ionize the iodine ions at reduced charge states, with some of them ending up in the lower enhancement region. This timing distribution of the charge rearrangement can also explain the iodine CSDs in Figs. 2(e) and 2(f) being in general smoother than those of xenon in the high charge state region above I^{25+}. Since charge transfer probability decreases with larger donor-acceptor distance, we expect to see a dependence of the resonance-enhancement features in the molecular CSDs on the pulse duration, because a certain charge state is on average reached at a larger internuclear distance with longer pulses [15]. A future study with different pulse durations could be an effective alternative to pump-probe experiments for investigating the charge transfer effect on resonance-enhanced ionization of molecules.

IV. CONCLUSION

In summary, resonance-enhanced x-ray multiple ionization, which was first discovered in high-Z atoms, is observed for molecular targets. The region of resonant enhancement shifts to higher charge states with increasing photon energy. The CSD of the heavy atom in the molecule resembles that of its atomic reference, but has distinct features which can be qualitatively explained by ultrafast charge rearrangement which can result in a charge state decrease for some of the ions initially in the major resonant-enhancement region. In addition, we demonstrated that the charge-rearrangement-enhanced ionization, previously discovered with hard x rays, is also important in the soft x-ray regime if the fluence is sufficiently high. The result can be used as benchmark data for modeling the interaction between intense x rays and molecules, which involves bound-bound transitions. It shows that for quantum systems larger than atoms, charge rearrangement between atomic sites can affect the resonant enhancement, which should be taken into account, e.g., in coherent imaging experiments where the creation of transient resonances is anticipated.

Data recorded for the experiment at the European XFEL are available at [42].

ACKNOWLEDGMENTS

This work is supported by the U.S. Department of Energy, Office of Science, Basic Energy Sciences, Chemical Sciences, Geosciences, and Biosciences Division, who supported X.L. under Grant No. DE-SC0019451 and A.R. and D.R. under Grant No. DE-FG02-86ER13491. We acknowledge European XFEL in Schenefeld, Germany, for x-ray free-electron laser beam time at the SQS instrument and would like to thank the staff for their assistance. R.D., M.S.S., K.F., T.J., and M.H. acknowledge support from Deutsche Forschungsgemeinschaft (DFG) via Sonderforschungsbereich 1319 (ELCH). M.I., V.M., and Ph.S. acknowledge funding from the Volkswagen foundation within a Peter Paul Ewald-fellowship. K.K. and M.M. acknowledge support by the Cluster of Excellence Advanced Imaging of Matter of the DFG, EXC 2056, Project ID 390715994. T.M. and M.M. acknowledge support by the DFG, German Research Foundation - SFB-925 - project 170620586.

[1] L. Young, E. P. Kanter, B. Krässig, Y. Li, A. M. March, S. T. Pratt, R. Santra, S. H. Southworth, N. Rohringer, L. F. DiMauro, G. Doumy, C. A. Roedig, N. Berrah, L. Fang, M. Hoener, P. H. Bucksbaum, J. P. Cryan, S. Ghimire, J. M. Glownia, D. A. Reis *et al.*, Femtosecond electronic response of atoms to ultra-intense x-rays, Nature (London) **466**, 56 (2010).

[2] H. Fukuzawa, S.-K. Son, K. Motomura, S. Mondal, K. Nagaya, S. Wada, X.-J. Liu, R. Feifel, T. Tachibana, Y. Ito, M. Kimura, T. Sakai, K. Matsunami, H. Hayashita, J. Kajikawa, P. Johnsson, M. Siano, E. Kukk, B. Rudek, B. Erk *et al.*, Deep Inner-Shell Multiphoton Ionization by Intense X-Ray Free-Electron Laser Pulses, Phys. Rev. Lett. **110**, 173005 (2013).

[3] M. Hoener, L. Fang, O. Kornilov, O. Gessner, S. T. Pratt, M. Gühr, E. P. Kanter, C. Blaga, C. Bostedt, J. D. Bozek, P. H. Bucksbaum, C. Buth, M. Chen, R. Coffee, J. Cryan, L. DiMauro, M. Glownia, E. Hosler, E. Kukk, S. R. Leone *et al.*, Ultraintense X-Ray Induced Ionization, Dissociation, and Frustrated Absorption in Molecular Nitrogen, Phys. Rev. Lett. **104**, 253002 (2010).

[4] B. Rudek, S.-K. Son, L. Foucar, S. W. Epp, B. Erk, R. Hartmann, M. Adolph, R. Andritschke, A. Aquila, N. Berrah, C. Bostedt, J. Bozek, N. Coppola, F. Filsinger, H. Gorke, T. Gorkhover, H. Graafsma, L. Gumprecht, A. Hartmann, G. Hauser *et al.*, Ultra-efficient ionization of heavy atoms by intense x-ray free-electron laser pulses, Nat. Photon. **6**, 858 (2012).

[5] B. Rudek, D. Rolles, S.-K. Son, L. Foucar, B. Erk, S. Epp, R. Boll, D. Anielski, C. Bostedt, S. Schorb, R. Coffee, J. Bozek, S. Trippel, T. Marchenko, M. Simon, L. Christensen, S. De, S.-i. Wada, K. Ueda, I. Schlichting *et al.*, Resonance-enhanced multiple ionization of krypton at an x-ray free-electron laser, Phys. Rev. A **87**, 023413 (2013).

[6] P. J. Ho, C. Bostedt, S. Schorb, and L. Young, Theoretical Tracking of Resonance-Enhanced Multiple Ionization Pathways in X-Ray Free-Electron Laser Pulses, Phys. Rev. Lett. **113**, 253001 (2014).

[7] B. Rudek, K. Toyota, L. Foucar, B. Erk, R. Boll, C. Bomme, J. Correa, S. Carron, S. Boutet, G. J. Williams, K. R. Ferguson, R. Alonso-Mori, J. E. Koglin, T. Gorkhover, M. Bucher, C. S. Lehmann, B. Krässig, S. H. Southworth, L. Young, C. Bostedt *et al.*, Relativistic and resonant effects in the ionization of heavy atoms by ultra-intense hard x-rays, Nat. Commun. **9**, 4200 (2018).

[8] M. Ilchen, T. Mazza, E. T. Karamatskos, D. Markellos, S. Bakhtiarzadeh, A. J. Rafipoor, T. J. Kelly, N. Walsh, J. T. Costello, P. O'Keeffe, N. Gerken, M. Martins, P. Lambropoulos, and M. Meyer, Two-electron processes in multiple ionization under strong soft-x-ray radiation, Phys. Rev. A **94**, 013413 (2016).

[9] R. Guichard, M. Richter, J.-M. Rost, U. Saalmann, A. A. Sorokin, and K. Tiedtke, Multiple ionization of neon by soft x-rays at ultrahigh intensity, J. Phys. B: At., Mol., Opt. Phys. **46**, 164025 (2013).

[10] B. Erk, D. Rolles, L. Foucar, B. Rudek, S. W. Epp, M. Cryle, C. Bostedt, S. Schorb, J. Bozek, A. Rouzee, A. Hundertmark, T. Marchenko, M. Simon, F. Filsinger, L. Christensen, S. De, S. Trippel, J. Küpper, H. Stapelfeldt, S. Wada *et al.*, Ultrafast Charge Rearrangement and Nuclear Dynamics Upon Inner-Shell Multiple Ionization of Small Polyatomic Molecules, Phys. Rev. Lett. **110**, 053003 (2013).

[11] B. Erk, D. Rolles, L. Foucar, B. Rudek, S. W. Epp, M. Cryle, C. Bostedt, S. Schorb, J. Bozek, A. Rouzee, A. Hundertmark, T. Marchenko, M. Simon, F. Filsinger, L. Christensen, S. De, S. Trippel, J. Küpper, H. Stapelfeldt, S. Wada *et al.*, Inner-shell multiple ionization of polyatomic molecules with an intense x-ray free-electron laser studied by coincident ion momentum imaging, J. Phys. B: At., Mol., Opt. Phys. **46**, 164031 (2013).

[12] B. Erk, R. Boll, S. Trippel, D. Anielski, L. Foucar, B. Rudek, S. W. Epp, R. Coffee, S. Carron, S. Schorb, K. R. Ferguson, M. Swiggers, J. D. Bozek, M. Simon, T. Marchenko, J. Küpper, I. Schlichting, J. Ullrich, C. Bostedt, D. Rolles *et al.*, Imaging charge transfer in iodomethane upon x-ray photoabsorption, Science **345**, 288 (2014).

[13] K. Motomura, E. Kukk, H. Fukuzawa, S.-i. Wada, K. Nagaya, S. Ohmura, S. Mondal, T. Tachibana, Y. Ito, R. Koga, T. Sakai, K. Matsunami, A. Rudenko, C. Nicolas, X.-J. Liu, C. Miron, Y. Zhang, Y. Jiang, J. Chen, M. Anand *et al.*, Charge and nuclear dynamics induced by deep inner-shell multiphoton ionization of CH_3 I molecules by intense x-ray free-electron laser pulses, J. Phys. Chem. Lett. **6**, 2944 (2015).

[14] A. Rudenko, L. Inhester, K. Hanasaki, X. Li, S. J. Robatjazi, B. Erk, R. Boll, K. Toyota, Y. Hao, O. Vendrell, C. Bomme, E. Savelyev, B. Rudek, L. Foucar, S. H. Southworth, C. S. Lehmann, B. Kraessig, T. Marchenko, M. Simon, K. Ueda *et al.*, Femtosecond response of polyatomic molecules to ultra-intense hard x-rays, Nature (London) **546**, 129 (2017).

[15] X. Li, L. Inhester, S. J. Robatjazi, B. Erk, R. Boll, K. Hanasaki, K. Toyota, Y. Hao, C. Bomme, B. Rudek, L. Foucar, S. H. Southworth, C. S. Lehmann, B. Kraessig, T. Marchenko, M. Simon, K. Ueda, K. R. Ferguson, M. Bucher, T. Gorkhover *et al.*, Pulse Energy and Pulse Duration Effects in the Ionization and Fragmentation of Iodomethane by Ultraintense Hard X Rays, Phys. Rev. Lett. **127**, 093202 (2021).

[16] K. Nass, L. Foucar, T. R. M. Barends, E. Hartmann, S. Botha, R. L. Shoeman, R. B. Doak, R. Alonso-Mori, A. Aquila, S. Bajt, A. Barty, R. Bean, K. R. Beyerlein, M. Bublitz, N. Drachmann, J. Gregersen, H. O. Jönsson, W. Kabsch, S. Kassemeyer, J. E. Koglin *et al.*, Indications of radiation damage in ferredoxin microcrystals using high-intensity x-fel beams, J. Synchrotron Radiat. **22**, 225 (2015).

[17] L. Galli, S.-K. Son, M. Klinge, S. Bajt, A. Barty, R. Bean, C. Betzel, K. R. Beyerlein, C. Caleman, R. B. Doak, M. Duszenko, H. Fleckenstein, C. Gati, B. Hunt, R. A. Kirian, M. Liang, M. H. Nanao, K. Nass, D. Oberthür, L. Redecke *et al.*, Electronic damage in S atoms in a native protein crystal induced by an intense x-ray free-electron laser pulse, Struct. Dyn. **2**, 041703 (2015).

[18] N. Rohringer and R. Santra, Resonant Auger effect at high x-ray intensity, Phys. Rev. A **77**, 053404 (2008).

[19] E. P. Kanter, B. Krässig, Y. Li, A. M. March, P. Ho, N. Rohringer, R. Santra, S. H. Southworth, L. F. DiMauro, G. Doumy, C. A. Roedig, N. Berrah, L. Fang, M. Hoener, P. H. Bucksbaum, S. Ghimire, D. A. Reis, J. D. Bozek, C. Bostedt, M. Messerschmidt *et al.*, Unveiling and Driving Hidden Resonances with High-Fluence, High-Intensity X-Ray Pulses, Phys. Rev. Lett. **107**, 233001 (2011).

[20] T. Mazza, M. Ilchen, M. D. Kiselev, E. V. Gryzlova, T. M. Baumann, R. Boll, A. De Fanis, P. Grychtol, J. Montaño, V. Music, Y. Ovcharenko, N. Rennhack, D. E. Rivas, Ph. Schmidt, R. Wagner, P. Ziolkowski, N. Berrah, B. Erk, P. Johnsson, C. Küstner-Wetekam *et al.*, Mapping Resonance Structures in Transient Core-Ionized Atoms, Phys. Rev. X **10**, 041056 (2020).

[21] A. C. LaForge, S.-K. Son, D. Mishra, M. Ilchen, S. Duncanson, E. Eronen, E. Kukk, S. Wirok-Stoletow, D. Kolbasova, P. Walter, R. Boll, A. De Fanis, M. Meyer, Y. Ovcharenko, D. E. Rivas, P. Schmidt, S. Usenko, R. Santra, and N. Berrah, Resonance-Enhanced Multiphoton Ionization in the X-Ray Regime, Phys. Rev. Lett. **127**, 213202 (2021).

[22] C. Weninger, M. Purvis, D. Ryan, R. A. London, J. D. Bozek, C. Bostedt, A. Graf, G. Brown, J. J. Rocca, and N. Rohringer, Stimulated Electronic X-Ray Raman Scattering, Phys. Rev. Lett. **111**, 233902 (2013).

[23] J. T. O'Neal, E. G. Champenois, S. Oberli, R. Obaid, A. Al-Haddad, J. Barnard, N. Berrah, R. Coffee, J. Duris, G. Galinis, D. Garratt, J. M. Glownia, D. Haxton, P. Ho, S. Li, X. Li, J. MacArthur, J. P. Marangos, A. Natan, N. Shivaram *et al.*, Electronic Population Transfer via Impulsive Stimulated X-Ray Raman Scattering with Attosecond Soft-X-Ray Pulses, Phys. Rev. Lett. **125**, 073203 (2020).

[24] U. Eichmann, H. Rottke, S. Meise, J.-E. Rubensson, J. Söderström, M. Agåker, C. Såthe, M. Meyer, T. M. Baumann, R. Boll, A. De Fanis, P. Grychtol, M. Ilchen, T. Mazza, J. Montano, V. Music, Y. Ovcharenko, D. E. Rivas, S. Serkez, R. Wagner *et al.*, Photon-recoil imaging: Expanding the view of nonlinear x-ray physics, Science **369**, 1630 (2020).

[25] N. Rohringer, D. Ryan, R. A. London, M. Purvis, F. Albert, J. Dunn, J. D. Bozek, C. Bostedt, A. Graf, R. Hill, S. P. Hau-Riege, and J. J. Rocca, Atomic inner-shell X-ray laser at 1.46 nanometres pumped by an X-ray free-electron laser, Nature (London) **481**, 488 (2012).

[26] P. J. Ho, B. J. Daurer, M. F. Hantke, J. Bielecki, A. Al Haddad, M. Bucher, G. Doumy, K. R. Ferguson, L. Flückiger, T. Gorkhover, B. Iwan, C. Knight, S. Moeller, T. Osipov, D. Ray, S. H. Southworth, M. Svenda, N. Timneanu, A. Ulmer, P. Walter *et al.*, The role of transient resonances for ultra-fast imaging of single sucrose nanoclusters, Nat. Commun. **11**, 167 (2020).

[27] R. D. Cowan, *The Theory of Atomic Structure and Spectra* (University of California Press, Berkeley, CA, 1981).

[28] R. D. Cowan, Atomic Structure Codes, http://www.tcd.ie/Physics/people/Cormac.McGuinness/Cowan/.

[29] J. M. Schäfer, L. Inhester, S.-K. Son, R. F. Fink, and R. Santra, Electron and fluorescence spectra of a water molecule irradiated by an x-ray free-electron laser pulse, Phys. Rev. A **97**, 053415 (2018).

[30] W. Decking *et al.*, A MHz-repetition-rate hard X-ray free-electron laser driven by a superconducting linear accelerator, Nat. Photon. **14**, 391 (2020).

[31] R. Dörner, V. Mergel, O. Jagutzki, L. Spielberger, J. Ullrich, R. Moshammer, and H. Schmidt-Böcking, Cold target recoil ion momentum spectroscopy: a 'momentum microscope' to view atomic collision dynamics, Phys. Rep. **330**, 95 (2000).

[32] J. Ullrich, R. Moshammer, A. Dorn, R. Dörner, L. Ph. H. Schmidt, and H. Schmidt-Böcking, Recoil-ion and electron momentum spectroscopy: reaction-microscopes, Rep. Prog. Phys. **66**, 1463 (2003).

[33] G. Kastirke, M. S. Schöffler, M. Weller, J. Rist, R. Boll, N. Anders, T. M. Baumann, S. Eckart, B. Erk, A. De Fanis, K. Fehre, A. Gatton, S. Grundmann, P. Grychtol, A. Hartung, M. Hofmann, M. Ilchen, C. Janke, M. Kircher, M. Kunitski *et al.*, Photoelectron Diffraction Imaging of a Molecular Breakup Using an X-Ray Free-Electron Laser, Phys. Rev. X **10**, 021052 (2020).

[34] G. Kastirke, M. S. Schöffler, M. Weller, J. Rist, R. Boll, N. Anders, T. M. Baumann, S. Eckart, B. Erk, A. De Fanis, K. Fehre, A. Gatton, S. Grundmann, P. Grychtol, A. Hartung, M. Hofmann, M. Ilchen, C. Janke, M. Kircher, M. Kunitski *et al.*, Double Core-Hole Generation in O_2 Molecules Using an X-Ray Free-Electron Laser: Molecular-Frame Photoelectron Angular Distributions, Phys. Rev. Lett. **125**, 163201 (2020).

[35] T. Jahnke, R. Guillemin, L. Inhester, S.-K. Son, G. Kastirke, M. Ilchen, J. Rist, D. Trabert, N. Melzer, N. Anders, T. Mazza, R. Boll, A. De Fanis, V. Music, Th. Weber, M. Weller, S. Eckart, K. Fehre, S. Grundmann, A. Hartung *et al.*, Inner-Shell-Ionization-Induced Femtosecond Structural Dynamics of Water Molecules Imaged at an X-Ray Free-Electron Laser, Phys. Rev. X **11**, 041044 (2021).

[36] X. Li, A. Rudenko, M. S. Schöffler, N. Anders, Th. M. Baumann, S. Eckart, B. Erk, A. De Fanis, K. Fehre, R. Dörner, L. Foucar, S. Grundmann, P. Grychtol, A. Hartung, M. Hofmann, M. Ilchen, Ch. Janke, G. Kastirke, M. Kircher, K. Kubicek *et al.*, Coulomb explosion imaging of small polyatomic molecules with ultrashort x-ray pulses, Phys. Rev. Research **4**, 013029 (2022).

[37] R. Boll, J. M. Schäfer, B. Richard, K. Fehre, G. Kastirke, Z. Jurek, M. S. Schöffler, M. M. Abdullah, N. Anders, T. M. Baumann, S. Eckart, B. Erk, A. De Fanis, R. Dörner, S. Grundmann, P. Grychtol, A. Hartung, M. Hofmann, M. Ilchen, L. Inhester *et al.*, X-ray multiphoton-induced Coulomb explosion images complex single molecules, Nat. Phys. **18**, 423 (2022).

[38] O. Jagutzki, A. Cerezo, A. Czasch, R. Dörner, M. Hattaß, M. Huang, V. Mergel, U. Spillmann, K. Ullmann-Pfleger, T. Weber, H. Schmidt-Bocking, and G. D. W. Smith, Multiple hit readout of a microchannel plate detector with a three-layer delay-line anode, IEEE Trans. Nucl. Sci. **49**, 2477 (2002).

[39] H. Ryufuku, K. Sasaki, and T. Watanabe, Oscillatory behavior of charge transfer cross sections as a function of the charge of projectiles in low-energy collisions, Phys. Rev. A **21**, 745 (1980).

[40] A. Niehaus, A classical model for multiple-electron capture in slow collisions of highly charged ions with atoms, J. Phys. B At., Mol., Opt. Phys. **19**, 2925 (1986).

[41] NIST Standard Reference Database 101, http://cccbdb.nist.gov/.

[42] See, https://doi.org/10.22003/xfel.eu-data-002159-00.